

Holistic Understanding of 3D Scenes as Universal Scene Description

Anna-Maria Halacheva^{1*}, Yang Miao^{1*}, Jan-Nico Zaech¹,
Xi Wang^{1,2}, Luc Van Gool^{1,2}, Danda Pani Paudel¹

¹INSAIT, Sofia University “St. Kliment Ohridski”, Bulgaria, ²ETH Zurich, Switzerland

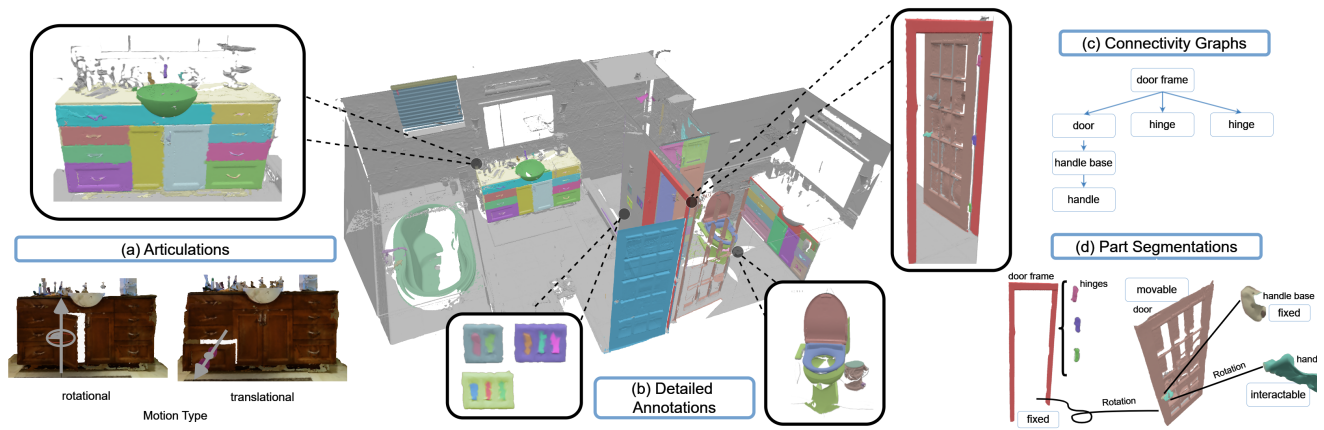


Figure 1. The **Articulate3D Dataset**. We introduce the first dataset to provide joint annotations on: (1) high-detail semantic segmentation at both the object and part levels, (2) part connectivity graphs, (3) part articulations, and (4) movable (articulated) parts and their corresponding interactable parts, which are used for interactions with the object (e.g., handles). Additionally, Articulate3D is the first large-scale dataset in USD format, facilitating efficient scene processing and expansion, as well as integration into robotic simulations.

Abstract

3D scene understanding is a long-standing challenge in computer vision and a key component in enabling mixed reality, wearable computing, and embodied AI. Providing a solution to these applications requires a multifaceted approach that covers scene-centric, object-centric, as well as interaction-centric capabilities. While there exist numerous datasets approaching the former two problems, the task of understanding interactable and articulated objects is underrepresented and only partly covered by current works. In this work, we address this shortcoming and introduce (1) an expertly curated dataset in the Universal Scene Description (USD) format, featuring high-quality manual annotations, for instance, segmentation and articulation on 280 indoor scenes; (2) a learning-based model together with a novel baseline capable of predicting part segmentation along with a full specification of motion attributes, including motion type, articulated and interactable parts, and motion parameters; (3) a benchmark serving to compare upcoming methods for the task at hand. Overall, our dataset

provides 8 types of annotations - object and part segmentations, motion types, movable and interactable parts, motion parameters, connectivity, and object mass annotations. With its broad and high-quality annotations, the data provides the basis for holistic 3D scene understanding models. All data is provided in the USD format, allowing interoperability and easy integration with downstream tasks. We provide [open access](#) to our dataset, benchmark, and method’s source code.

1. Introduction

With 3D scene understanding, computer vision enables an important capability for downstream applications in mixed reality, wearable computing and embodied AI. Across all of these applications, understanding is performed with different semantic levels and planning horizons: in a semantic context, scene understanding covers mapping of 3D environments for navigation, detection of objects in 2D and 3D,

*Equal contribution

fine-grained segmentation of parts for semantics, their connectivities and functionalities.

To facilitate the diverse aforementioned tasks, we propose to perform 3D scene understanding in the Universal Scene Description (USD) format. Representing 3D scenes in this format enables seamless interoperability, modular scene composition, and efficient rendering. USD is an ideal representation for the physics simulation of both static and animated scenes. However, converting real 3D scenes into this format comes with several challenges. In this paper, we address two key challenges in this regard by offering: (1) expert annotation and curation of a large-scale real-world dataset in USD, Articulate3D, and (2) a method to effectively address different aspects required to automatically convert a given 3D scan into a usable USD format.

To create simulation-ready scenes in USD, we provide multi-level annotations. As illustrated in Fig. 1, our dataset includes: (1) semantic instance segmentations on both object and part level, (2) their connectivity, (3) the articulations within the scenes, and (4) the articulation role of the parts within the part segmentations. Our dataset offers the most extensive articulation annotations available for 3D indoor scenes, covering all aspects necessary for realistic articulation simulation. We label the motion type, the motion parameters, as well as the role of the different parts within the articulated structure. We annotate both the *movable* parts, as well as the *interactable* ones used to interact with the object, e.g. handle as an interactable part for the movable door. Additionally, we specify fixed attachments between parts and objects, for example, a door frame attached to a wall or a handle base fixed to a door.

Our annotation categories make Articulate3D the richest scene articulation dataset, providing more extensive information for holistic 3D scene understanding, as highlighted in Tab. 1. Numerous 3D indoor scene datasets have been introduced, but most focus only on semantic segmentation at the object level [2, 8, 14, 62, 73]. Among existing datasets, SceneFun3D [9] and MultiScan [29] incorporate articulation annotations, though at a limited scale. SceneFun3D provides detailed labels for interactable parts (e.g., handles, buttons) across various categories, but lacks segmentation and articulation for all movable parts, as well as object-level segmentation. MultiScan, while covering a broader range of categories, offers lower scan quality and incomplete articulation data, with limited specifications on interactability. To address these limitations and support advanced scene understanding, we present Articulate3D, annotated across the 8 categories essential for physical simulations: semantic instance segmentation at both object and part levels, motion types, movable and interactable parts, motion parameters, connectivity, and object mass.

Based on Articulate3D, we further propose a benchmark with a full specification of motion attributes, includ-

ing the task of movable part segmentation, motion type prediction, articulation parameters prediction, and interactable part segmentation. A baseline capable of implementing the benchmark tasks is built by adapting a recent 3D instance segmentation framework [49]. Based on the baseline, we further propose the point-wise dense prediction mechanism which significantly improves the performance of articulation prediction (by 7.3% over baseline for articulation origin prediction).

Overall, this work makes the following contributions:

- The richest articulation dataset for real-world 3D scenes, combining semantic part and object instance segmentations, connectivity, and detailed articulation annotations. Articulate3D is also the first large-scale, non-synthetic USD dataset.
- A method for 3D movable part segmentation, motion type, articulation prediction, and interaction segmentation for 3D scene point clouds.
- A systematic benchmark of methods for agent-oriented scene understanding tasks in 3D mobility segmentation, articulation prediction, and interaction segmentation

2. Related Work

We provide an overview of related work on datasets for semantic scene understanding and 3D object articulation, offering a summarized overview in Tab. 1. Additionally, we review existing algorithms for holistic scene understanding. **Dataset - 3D Semantic Understanding** is crucial for various downstream tasks, such as mixed reality scene generation and editing [23, 37, 63, 66, 75], scene reasoning via interactive agents [10, 15], or embodied AI applications [41, 48, 71]. Advancing research in these fields requires datasets with high-quality scans as well as detailed, multimodal annotations [4, 13, 28]. For example, embodied AI applications require precise articulation data, and simulation learning relies on annotated physical properties. A shared foundation for many of these tasks is robust semantic instance segmentation. In response, various 3D scene datasets have been introduced. ScanNet++ [73], ScanNet [8], Matterport3D [2] and others [14, 62, 68] offer instance segmentation with extensive label details. Another branch prioritizes high-definition scans and scale but provides very limited to no annotations, e.g. ARKitScenes [1] and HM3D [44]. Others balance data volume and annotation quality by including thousands of scenes with automated annotations and incorporation of synthetic data [18, 64]. While useful for large-scale tasks, the synthetic-real gap can affect model performance [60, 70].

Despite the diversity in available datasets, most provide a single annotation type and offer only object-level semantic segmentation [2, 8, 14, 62, 68, 73], limiting their applicability for tasks requiring finer detail. Although datasets with both object- and part-level annotations exist [30], those con-

Dataset	Instance		Articulation			Connectivity	HD-3D	USD
	Object	Part	Motion-Param	Movable	Interactable			
SceneNN [14]	✓	✗	✗	✗	✗	✗	✗	✗
Replica [54]	✓	✗	✗	✗	✗	✗	✗	✗
ScanNet [8]	✓	✗	✗	✗	✗	✗	✗	✗
Matterport3D [2]	✓	✗	✗	✗	✗	✗	✗	✗
ARKitScenes [1]	✗	✗	✗	✗	✗	✗	✓	✗
ScanNet++ [73]	✓	✗	✗	✗	✗	✗	✓	✗
3RScan [62]	✓	✗	✗	✗	✗	✗	✗	✗
SceneFun3D [9]	✗	✓	✓	✗	✓	✗	✓	✗
MultiScan [29]	✓	✓	✓	✓	✗	✓	✗	✗
Articulate3D(Ours)	✓	✓	✓	✓	✓	✓	✓	✓

Table 1. Comparison of 3D indoor scene datasets. Articulate3D is the first dataset to combine high-quality real-world scene scans, instance segmentations on both object and part-level, connectivity and all articulation annotation types necessary to execute/simulate an interaction with an object. Articulate3D offers all those annotations within the adopted USD format as the first large-scale USD dataset. Articulate3D not only offers the most types of annotations, but also provides them on high-definition scenes (HD 3D).

sist of isolated objects rather than complete scenes, reducing their suitability for holistic 3D scene understanding.

Articulate3D addresses these gaps by providing high-definition 3D scans with label-rich object- and part-level segmentation, as well as connectivity graphs, mass annotations, and extensive articulation data, creating a foundation for advanced 3D scene understanding.

Dataset - 3D Articulation Information is essential for 3D scene understanding, enabling realistic object manipulation and interaction. Recent research on learning articulation patterns [20, 24, 53] and representing articulated states [25, 42, 56], showing the need for richly-annotated articulation datasets to support tasks requiring dynamic scene exploration and interaction. Recent datasets have expanded the scope of object articulation annotations, but still lack the full details needed for comprehensive representation, e.g. in a simulation. SceneFun3D [9] adds interactable parts segmentation and their articulation data to ARKitScenes but lacks complete object instance segmentation and connectivity annotations for scene understanding. MultiScan [29] provides part-level articulations and segmentations but not the interactable components necessary for practical manipulation. Its mobility annotations also rely on multiple scans of objects in different states, complicating processing and extensibility. Other datasets annotate articulation

parameters and movable, interactable parts but include only individual objects [26, 67], limiting their use for full-scene tasks. Finally, RoboCasa [31] offers articulation annotations within synthetic environments, but the synthetic setting introduces a domain gap.

Our dataset addresses these limitations by providing a broad set of annotation types, covering movable and interactable parts, and precise movement specifications (Tab. 1). Provided in USD format, our annotations allow for simulation-ready scenes without multiple scans. Through the format we also ensure easy adaptability and extensibility, as well as integration into robotics and embodied AI workflows with USD as requested format [32, 60].

Algorithms - Holistic Scene Understanding involves recognizing objects, their spatial relationships, articulations and contextual information about the scene as a whole. We focus on part-level segmentation and articulation within indoor scenes. One popular approach is 2D image-based methods [6, 19, 27, 55, 58, 74] that use RGB(-D) images for 2D/3D part-level scene understanding tasks. [19, 55] address the task of detecting openable part detection and their 3D motion parameters from a single image, while [6, 27, 74] focus on object-part-level understanding in 2D. However, those methods are limited to single objects or small-scale scenes due to the restricted viewpoint of images. 3D-based methods offer an alternative by directly processing 3D data to achieve holistic scene understanding. Pioneered by [3, 5, 12], research in 3D semantic/instance scene understanding has gained popularity [3, 46, 49, 57, 61, 72]. Meanwhile, due to lack of high-quality 3D dataset with complete articulations, 3D holistic scene understanding of articulation is still an open problem. Recently, there has been growing interest in developing methods that capture the articulation intricacies [9, 29, 51, 52, 65, 69]. However, those methods either focus on single object parsing with synthetic data, or on partial articulation prediction, limiting their applications in real-world scenarios. To address this, we build a baseline using recent 3D instance segmentation frameworks, such as [49] and [61], with verified performance and publicly available code.

3. Universal Scene Description

Choosing Universal Scene Description (USD) for Articulate3D ensures both high industry standards and advanced research compatibility. Developed by Pixar and now an open-source standard, USD offers information-rich scene representations and easy integration with advanced simulation tools. Below, we introduce the format and its benefits.

3.1. USD Format

USD organizes a scene into hierarchical entities, primitives (prims)—the building blocks representing all objects and relationships in the scene. Prims support a nested structure,

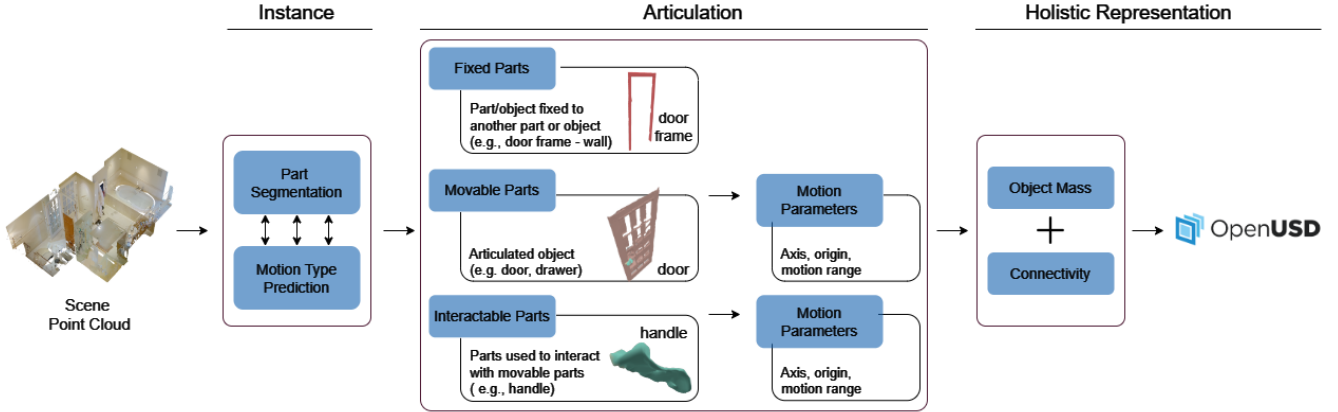


Figure 2. Overview of the annotations provided in Articulate3D, leading us to the creation of USD scene representations. We determine the objects and their parts. We annotate motion type (rotational, translational, none), and based on it - the articulations. We identify the role of the different parts within the articulations (movable or interactable). For each articulated part we also capture the motion parameters axis, origin (only for rotation) and motion range, or a fixture point for fixed objects. We use the annotated connectivity information to build the full USD file, also enhancing it with object mass labels for physical simulation support.

where complex objects (e.g., cabinets) are represented as parent prims containing child sub-prims, modeling both individual items and grouped components of the scene.

Each prim can be assigned various attributes, e.g., position, scale, orientation, geometry, and appearance. Custom attributes can be introduced, enabling dataset-specific data to be embedded directly within the scene, such as physical properties (e.g., mass), material details, or semantic labels.

USD also supports joints that define movable connections, e.g., door hinges, as well as fixed joints. This enables the representation of both fixed and dynamic object relationships, making USD particularly suited for applications requiring detailed articulation and interaction modeling.

3.2. Benefits of the USD Format

USD offers a highly robust, standardized format for representing complex 3D scenes, making it an ideal choice for Articulate3D. It supports rich 3D data representations, including mesh geometry, semantic segmentations, connectivity and articulation definitions, and physical attributes - all within a single, unified file. It offers an efficient, lightweight alternative to datasets like MultiScan [29], which require multiple scans of articulated objects in their open and closed states. USD’s structure also supports non-destructive edits, facilitating scene manipulations.

USD also offers extensive tool support like the `usd-core` library for Python, making it accessible and easy to integrate with common workflows, alleviating the need for custom data loaders, and merging information from multiple annotation files. Additional AI-powered tools by NVIDIA, such as USD Code [35] for code generation and USD Search [36] for easy asset search, simplify both the creation and management of large-scale 3D environments. We further demonstrate that LLMs are able to understand USD

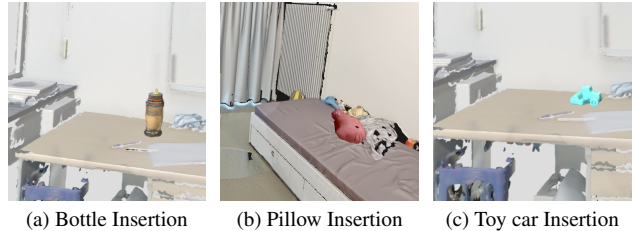


Figure 3. Visualizations of scenes from Articulate3D, after object insertion via LLM on our annotated USD files.

files and generate code for automatic object insertion into USD scenes. When prompted to place objects in USD scenes, the LLMs not only produced correct insertion code but also identified appropriate semantic locations for the objects (e.g., placing a pillow on a bed), as shown in Fig. 3. This showcases that the USD format’s rich and extensible structure enables LLMs to effectively interpret and manipulate complex 3D scenes, otherwise impossible with other dataset formats like PLY or JSON.

USD’s relevance and utility are increasingly recognized within the research community. NVIDIA’s Isaac Sim [34], built on USD, is gaining popularity as the state-of-the-art simulator for research with its high-fidelity environment for realistic physics-based simulations [17, 21, 45, 60, 76]. USD is also widely used in research going beyond robotics simulations for projects like procedural scene generation [43] and knowledge graph conversion for semantic querying [32].

4. Building the Articulate3D Dataset

In this section, we detail the construction of our dataset, Articulate3D, which builds upon the ScanNet++ dataset [73] by adding part-level annotations, articulation information, part connectivity, and object mass annotations, enabling a

holistic representation in USD (OpenUSD) format, as illustrated in Fig. 2. Our work uses the high-quality data and dense semantic annotations of ScanNet++ as a foundation, upon which we layer additional annotations for enhanced scene understanding and interaction modeling.

4.1. ScanNet++ as a Foundation

ScanNet++ [73] provides 380 richly annotated 3D scenes captured using a Faro Focus Premium laser scanner, producing sub-millimeter resolution point clouds with an average size of 40 million points. Additionally, it includes registered RGB-D streams and high-resolution DSLR images for each scene. This multi-source data collection strategy makes the dataset suitable for tasks that integrate 2D and 3D information, following recent trends in the scene understanding field [16, 33, 40, 57]. The alignment between the RGB-D data, DSLR images, and laser-scanned point clouds is consistently reported to be accurate, making ScanNet++ one of the highest-quality datasets available.

Choice of ScanNet++ over other datasets (e.g., MultiScan [29], ScanNet [8], Matterport3D [2], Tanks and Temples [22], ETH3D [50]) is based on its (1) superior data resolution, (2) extensive laser scan coverage, and (3) dense semantic annotations. Notably, while ARKitScenes [1] offers comparable mesh quality, it does not provide semantic segmentations, making ScanNet++ the only ideal basis for the complex annotations needed in Articulate3D.

Our work focuses on the 280 training scenes from ScanNet++, as the 50 validation and 50 test scenes are only available in point cloud format without object-level semantic annotations. This subset of fully labeled scenes provides the necessary foundation for detailed part-level, connectivity, and articulation annotations in Articulate3D.

4.2. Building Articulate3D

The Articulate3D dataset introduces new layers of annotation onto ScanNet++’s base. Our annotation process covers part segmentation, articulation, part connectivity, and physical properties, each designed to enhance scene understanding. Fig. 2 provides an overview of the different annotation categories and their associated parameters. In addition to articulating the properties of movable parts, such as motion type, axis, origin, and range, we also annotate the interactable parts that facilitate interaction, e.g., handles for doors. Furthermore, fixed attachments between parts and objects, as well as the mass of non-fixed objects, are also provided to support physical simulations.

To ensure consistency across scenes, our annotation approach defines a standardized set of 50 objects, including items like cabinets, windows, heaters, ovens, etc., and specifies the parts within each object to be segmented. We annotate overall 70 part classes. A complete list of the 120 labels of the objects with the possible associated parts, together

with the label distribution, is provided in the supplementary. Within these labels, we allow for some flexibility to capture nuanced semantics. For instance, a "cabinet" may be labeled as "cabinet" or "closet" based on its appearance or location. Functional distinctions are also incorporated, such as labeling faucet parts as either "faucet control" or "faucet handle". This approach ensures broad semantic coverage while preserving subtle distinctions that may be valuable for downstream tasks. We note that label synonyms are not counted as additional object classes; for instance, while "trash bin" may appear as "trash bin" or "trash can", only "trash bin" is counted among the 50 defined object labels. A list with the used synonyms and label variations will be released within the dataset.

To ensure thorough and accurate annotation, each scene undergoes a two-stage process. The annotation pipeline is based on MultiScan’s annotation tools with extensions to support connectivity annotation, additional filters for motion types, and refined articulation suggestions. In the first stage, annotators focus on part segmentation and connectivity annotations. The connectivity is provided through hierarchical connectivity graphs with the "root" being the base to which other parts are attached. A "child" refers to a part that belongs to the object, either through physical attachment (e.g., a door attached to a cabinet or a handle affixed to a door) or functional association (e.g., a lid of a container box, which is fully detachable but still part of the object by its intended function or use). This is followed by a second stage, where articulation properties are annotated, capturing motion type, axis, origin, and range, as shown in Fig. 2.

Our team consists of five expert annotators who conduct the primary annotations, followed by a sixth expert who reviews and refines all submitted annotations. This quality control step is critical in maintaining consistency and accuracy across the dataset.

Part Segmentation and Connectivity Our part segmentation process involves manual annotation by expert annotators, who segment and label the parts of the fixed set of objects, and then establish part connectivity. To enhance accuracy, we provide annotators with additional oversegmentation of the objects with ScanNet++ object class labels relevant to our annotations (e.g., doors, windows, cabinets, fridges, ovens). To obtain this oversegmentation, we use Felzenszwalb and Huttenlocher’s hierarchical graph-based segmentation algorithm [11].

The oversegmentation divides the mesh into smaller, manageable segments, with the coarse level capturing larger parts and the fine level delineating finer boundaries based on individual triangles. This enables annotators to use pre-segmented boundaries as a starting point, significantly speeding up the annotation process. Where appropriate, annotators can refine these segments to capture smaller details or make adjustments when the automated segmenta-

tion is imprecise. This approach ensures that even intricate parts are accurately labeled, while minimizing the number of points left unannotated and capturing clear object boundaries. Additionally, in cases where the oversegmentation does not provide adequate granularity, annotators can label directly at the triangle level. This fine-granular approach is essential for addressing inaccuracies within ScanNet++’s original semantic segmentation in certain scenes.

To ensure the quality of the connectivity annotations, we implement automated checks that detect annotation issues. These checks identify instances of double-parenting and detect any gaps in the hierarchy, alerting annotators to inconsistencies or errors. This combination of expert review and automated validation ensures that even the complex annotations meet our high standards for accuracy and consistency, resulting in a dataset that is both detailed and reliable.

Articulation Annotation For each part we annotate its role within its articulation structure - movable, interactable, with a fixed attachment, or none. For the movable parts, the annotators label the base part (the stationary reference), movement type (either translational or rotational), axis, movement origin, and movement restrictions (angle limits for rotation or distance limits for translation), as shown in Tab. 1.

To annotate articulations, we provide annotators with semi-automated suggestions. For hinge-based rotations (e.g., doors, windows), we estimate the rotation axis along the longest vertical edge of the bounding box. For sliding parts (e.g., drawers), we use surface normals from the object’s front face to predict the translation axis. These predictions offer an initial guide that annotators refine as needed, ensuring accurate and efficient labeling of movable parts. Fixed articulations are also introduced to represent immovable fixtures, such as ceiling lights attached to ceilings or door frames anchored to walls. To determine which objects can be fixtures, we define a set of eligible class labels. Within each scene, candidates for a fixture are proposed based on the proximity of bounding boxes and an example attachment point of closest proximity to the two objects is determined. Annotators verify and refine these suggested connections, ensuring accurate and consistent labeling.

Mass Annotation We assign a predefined mass to each object class. To estimate the mass of individual instances, we scale the class mass according to the volume of each instance’s bounding box. This approach provides instance-specific weight estimates, enabling realistic physical simulations and enhancing scene understanding.

Conversion to USD Format To facilitate ease of use and adaption, as well as integration with simulation platforms, we export Articulate3D in Universal Scene Description (USD) format. Using the USD-core library, we programmatically convert our annotated scenes, including ScanNet++’s dense semantic segmentation and our part-level and articulation annotations.

4.3. Articulate3D Statistics

Our dataset includes annotations on 8 different categories - object and part segmentations, motion types, movable and interactable parts, motion parameters, connectivity and object mass annotations. Our semantic segmentations cover 120 label classes - 50 object classes and 70 part classes. Detailed label lists, along with lists of synonyms within the dataset (not counted in the 120 labels), and label distribution information are provided in the supplementary material.

On average, we enhance each scene with 45 segmentations and 11 hierarchies, with the hierarchy depth averaging 4 parts, including the root part. Our segmentations on average cover 25% of the mesh vertices in each scene, excluding the background elements such as the floor, walls, and ceiling. On the articulation level, Articulate3D includes 21 articulations per scene on average, with $\approx 70\%$ being rotational.

5. Benchmarks and Experiments

We illustrate the value of Articulate3D dataset on the following tasks: (1) Movable Part Segmentation, (2) Articulation Parameter Prediction, and (3) Interaction Part Segmentation. We build the baseline on the codebase of state-of-the-art methods that have public code and verified performance on 3D instance segmentation task on ScanNet [8] and Scannet++ [73] benchmarks and evaluate them on the 3 tasks above on Articulate3D. Additional implementation details and experiments can be found in the supplementary.

5.1. Preliminary

As illustrated in Sec 4.2, the parts of articulated objects can be movable, interactable or fixed. For each movable part, we predict its articulation parameters including motion type (rotation and translation), motion axis and origin. In experiments, we assume each movable part has descendant interactable part in the connectivity graph and exclude movable parts without interaction (i.e. drawer without handle due to incomplete 3D reconstruction or touch-latch cabinet door).

5.2. Method

As representative approaches from distinct methodological branches, Softgroup [61] and Mask3D [49] are adapted as baselines in our evaluation. For clarity, we denote these adapted baselines as SoftGroup[†] and Mask3D[†]. In addition, we introduce ArtMask3D, a novel framework that leverages dense articulation prediction to achieve superior performance on the benchmark.

SoftGroup[†]. For instance segmentation of movable and interactable parts, SoftGroup[†] directly re-uses the network of SoftGroup. For articulation parameters, SoftGroup[†] takes the segmentation of movable parts and aggregates per-instance backbone features for the prediction via an addi-

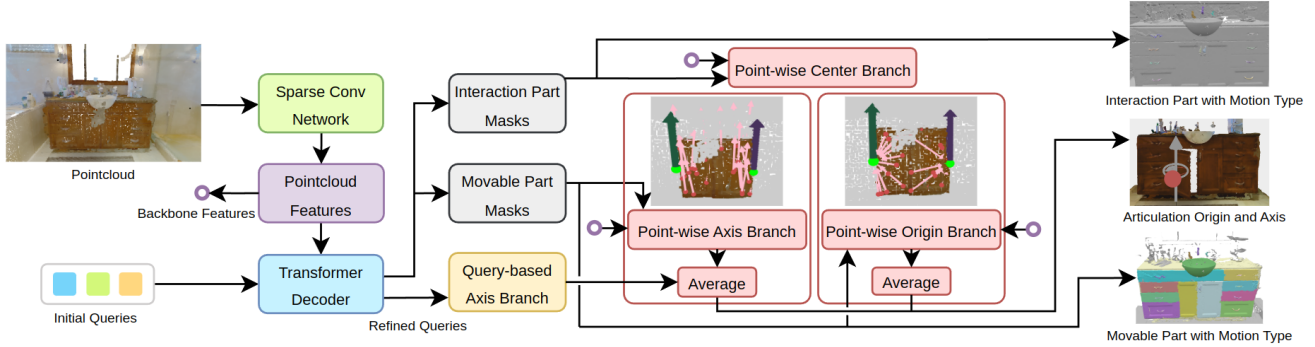


Figure 4. Framework of ArtMask3D for movable/interactable part segmentation, motion type classification, and articulation prediction.

tional origin and axis prediction branches. More implementation details can be found in supplementary results.

Mask3D[†]. We apply Mask3D for movable and interactable part segmentation with its original 3D instance segmentation framework. For articulation parameter prediction, inspired by OPDMulti [55] and SceneFun3D [9], we add an additional head that maps the per-part instance queries to articulation predictions.

ArtMask3D. We develop ArtMask3D for the proposed benchmarks, as shown in Fig. 4. Compared to Mask3D[†], instead of merely using the instance queries for articulation prediction, we leverage the per-instance pointcloud backbone features for dense prediction of articulation parameters. Specifically, for each point in the predicted movable part, ArtMask3D maps its feature vector to the offset from the point to the articulation origin, predicting the point-wise origin in local part coordinates. Then, point-wise origins are averaged over all points within the corresponding predicted movable part mask for origin prediction. For the axis prediction, we utilize both point-wise and query-based prediction, applying the point-wise averaging afterward.

We compare SoftGroup[†], Mask3D[†], and ArtMask3D in the following tasks with same experimental settings.

5.3. Movable Part Segmentation

For a scene point cloud, we predict instances $M = \{m_k\}_{k=1}^K$ of movable parts. Per movable part m_k , we also predict the motion type $C = \{c_k \in \{\text{background, rotation, translation}\}\}$.

Implementation. Given the many small movable parts (e.g., buttons, switches) in Articulate3D, we apply the coarse-to-fine learning strategy from SceneFun3D [9] for all three methods during training. For SoftGroup[†], we first train with only semantic loss, then apply the instance grouping loss while keeping the backbone fixed. For Mask3D[†] and ArtMask3D, we first train the networks with movable part segmentation and motion type classification and after convergence add articulation loss. For all the 3 methods, we jointly predict the movable part segmentation and the articulation. For more implementation details, please refer

Method	AP	AP_{50}	AP_{25}
SoftGroup [†]	22.7	32.7	37.2
Mask3D [†] (baseline)	18.1	39.1	58.9
ArtMask3D (ours)	19.8	41.8	59.9

Table 2. Segmentation of movable part on Articulate3D.

to supplementary material.

Metric. To evaluate the 3D part segmentation and motion type classification accuracy, we report the mean average precision (AP) and AP with IoU thresholds of 0.25 (AP_{25}) and 0.5 (AP_{50}).

Result. The performance of the benchmarked methods, reported in Tab. 2, is the highest for ArtMask3D both for AP_{50} and AP_{25} . SoftGroup[†] shows the lowest AP_{50} and AP_{25} but the highest AP , due to the IoU prediction branch in [61], which filters out false positive instance proposals. In contrast, Mask3D-based methods are prone to overconfident predictions, as instance confidence is directly estimated from category and mask scores.

5.4. Articulation Prediction

Using the movable part segmentation, we predict the articulation parameters of movable parts. For a point cloud and obtained movable part segmentations M , we predict the motion origin $\{o_k \in \mathbb{R}^3\}$ and motion axis $\{a_k \in \mathbb{R}^3\}$ for the articulation per movable part m_k .

Implementation. In [9, 29, 55], $L1$ loss is applied to supervise the network to predict the same origin and axis as the ground truth annotations ($\{o_k^*, a_k^*\}$), making the training prone to noisy annotations (i.e. the origin of the same type of movable instances varies). For translational movements, the articulation axis is sufficient to describe the motion pattern, while rotational ones also require origin specification. Thus, we apply category-specific articulation loss. For translation parameters, we only consider the axis loss, formulated as the cos-dissimilarity between the predicted axis and the ground truth. For rotation, we consider cos-dissimilarity for axis prediction and the perpendicular distance between the rotation center and the axis.

Metric. Inspired by [9], we extend AP_{50} with our own

Method	AP_{50}		
	+Origin	+Axis	+Origin+Axis
SoftGroup [†]	18.5	21.5	17.7
Mask3D [†] (baseline)	24.4	33.8	19.3
ArtMask3D (ours)	31.4	34.6	25.0

Table 3. Articulation parameters of movable part on Articulate3D.

Method	AP	AP_{50}	AP_{25}
SoftGroup [†]	6.8	14.5	25.4
Mask3D [†] (baseline)	12.7	30.2	55.6
ArtMask3D (ours)	12.7	31.1	55.9

Table 4. Segmentation of interaction part on Articulate3D.

category-specific articulation loss to jointly evaluate the accuracy of the predicted movable part segmentation and of the predicted articulation parameters. As shown in Table 3, $AP_{50} + \{\text{Axis}, \text{Origin}\}$ represents that a prediction is considered as true positive only when (1) the iou between part segmentation and G.T. mask is greater than 50%, and (2) the articulation loss is below certain threshold.

Result. Table 3 shows that ArtMask3D achieves significantly better performance than the baselines in prediction of both articulation parameters by a significant margin (surpassing SoftGroup[†] by 7.3% and Mask3D[†] by 5.7% for $AP_{50} + \text{Axis} + \text{Origin}$). As illustrated in later ablation study and supplementary material, the advantage of ArtMask3D lies in the dense articulation prediction that helps localization of articulation in the local coordinate system, as introduced in Sec. 5.2.

5.5. Interaction Part Segmentation

For a scene point cloud, we predict segmentation of interactable parts $I = \{i_k\}_{k=1}^L$ and for each i_k its motion type label $t_k \in \{\text{rotation}, \text{translation}\}$. We apply the coarse-to-fine learning strategy mentioned in Sec. 5.3 to facilitate the segmentation of the usually small interaction parts.

Metric. We report the mean average precision (AP) and AP with IoU thresholds of 0.25 (AP_{25}) and 0.5 (AP_{50}) for measuring accuracy of interaction part segmentation.

Result. Table 4 shows that ArtMask3D performs better than Mask3D[†], illustrating the effectiveness of the point-wise center branch for interaction part predictions as shown in Fig/ 4. It is noticeable that SoftGroup[†] performs inferior to ArtMask3D and Mask3D[†], which is in accordance with the benchmarks of [7, 9, 73].

5.6. Additional Experiments

We show the effectiveness of the proposed method and the value of our dataset via additional experiments.

Ablation Study. To further understand the effectiveness of the dense point-wise prediction mechanism in ArtMask3D, we implement ablations as shown in Table 5. The table il-

Method	AP_{50}		
	+Origin	+Axis	+Origin+Axis
Mask3D [†] (wo. both)	24.4	33.8	19.3
wo. dense axis	26.9	30.3	21.9
wo. dense origin	21.1	38.7	18.2
ArtMask3D	31.4	34.6	25.0

Table 5. Ablations on dense articulation prediction mechanism.

Settings	AP_{50}	+Origin	+Axis	+Origin+Axis
wo. pretrain	34.8	28.1	30.1	24.3
w. pretrain	40.5	31.3	33.8	26.0

Table 6. Evaluation of ArtMask3D on Multiscan [29] without and with pre-training on Articulate3D.

lustrates that (1) without the dense prediction of axis articulation, both origin and axis prediction performance drop; (2) without the dense prediction of origin, the axis prediction benefits but the origin prediction is significantly affected, resulting in significant decrease performance in joint articulation prediction evaluation; (3) with both dense prediction mechanism, ArtMask3D achieves the best joint articulation prediction accuracy.

Finetuning. To show the benefits of Articulate3D for the tasks in other datasets, we pretrain ArtMask3D on Articulate3D and finetune it on MultiScan for the movable part segmentation and articulation parameter prediction. In Table 6, we can see that by pretraining on Articulate3D, we can improve the performance of ArtMask3D in both tasks of movable part segmentation and articulation prediction.

6. Conclusion

We present Articulate3D, a dataset of 280 high-quality scans of real-world indoor scenes, annotated with semantic segmentations at the object and part levels, as well as articulation, connectivity, and object mass information. Articulate3D provides the most comprehensive set of articulation annotation categories to date, through specification of motion types, motion parameters, movable, interactable and fixed parts. As the first large-scale, non-synthetic dataset in USD format, Articulate3D also supports physical scene simulation. We demonstrate the benefits of the USD format showing how LLMs can be used for automatic object insertion into USD scenes.

To demonstrate Articulate3D’s quality and utility, we introduce a novel baseline for part segmentation and articulation prediction, along with a learning-based model that extends this baseline through a point-wise dense prediction mechanism for enhanced articulation predictions. We also establish a benchmark for these tasks. Together, our dataset and models set a new foundation for advancements in holistic scene understanding, with a deeper focus on object interactions.

Acknowledgments

This research was partially funded by the Ministry of Education and Science of Bulgaria (support for INSAIT, part of the Bulgarian National Roadmap for Research Infrastructure).

References

- [1] Gilad Baruch, Zhuoyuan Chen, Afshin Dehghan, Yuri Feigin, Peter Fu, Thomas Gebauer, Daniel Kurz, Tal Dimry, Brandon Joffe, Arik Schwartz, and Elad Shulman. ARK-scenes: A diverse real-world dataset for 3d indoor scene understanding using mobile RGB-d data. 2021. [2](#), [3](#), [5](#)
- [2] Angel Chang, Angela Dai, Thomas Funkhouser, Maciej Halber, Matthias Niebner, Manolis Savva, Shuran Song, Andy Zeng, and Yinda Zhang. Matterport3d: Learning from rgb-d data in indoor environments. In *International Conference on 3D Vision (3DV)*, 2017. [2](#), [3](#), [5](#)
- [3] R. Qi Charles, Hao Su, Mo Kaichun, and Leonidas J. Guibas. Pointnet: Deep learning on point sets for 3d classification and segmentation. In *International Conference on Computer Vision and Pattern Recognition (CVPR)*, 2017. [3](#), [15](#)
- [4] Hao Chen, Yuqi Hou, Chenyuan Qu, Irene Testini, Xiaohan Hong, and Jianbo Jiao. 360+x: A panoptic multi-modal scene understanding dataset. In *International Conference on Computer Vision and Pattern Recognition (CVPR)*, 2024. [2](#)
- [5] Shaoyu Chen, Jiemin Fang, Qian Zhang, Wenyu Liu, and Xinggang Wang. Hierarchical aggregation for 3d instance segmentation. In *International Conference on Computer Vision (ICCV)*, 2021. [3](#)
- [6] Xianjie Chen, Roozbeh Mottaghi, Xiaobai Liu, Sanja Fidler, Raquel Urtasun, and Alan Yuille. Detect what you can: Detecting and representing objects using holistic models and body parts. In *International Conference on Computer Vision and Pattern Recognition (CVPR)*, 2014. [3](#)
- [7] Angela Dai, Angel X. Chang, Manolis Savva, Maciej Halber, Thomas Funkhouser, and Matthias Nießner. Scannet: Richly-annotated 3d reconstructions of indoor scenes. In *International Conference on Computer Vision and Pattern Recognition (CVPR)*, 2017. [8](#)
- [8] Angela Dai, Angel X. Chang, Manolis Savva, Maciej Halber, Thomas Funkhouser, and Matthias Nießner. Scannet: Richly-annotated 3d reconstructions of indoor scenes. In *International Conference on Computer Vision and Pattern Recognition (CVPR)*, 2017. [2](#), [3](#), [5](#), [6](#)
- [9] Alexandros Delitzas, Ayca Takmaz, Federico Tombari, Robert Sumner, Marc Pollefeys, and Francis Engelmann. SceneFun3D: Fine-Grained Functionality and Affordance Understanding in 3D Scenes. In *International Conference on Computer Vision and Pattern Recognition (CVPR)*, 2024. [2](#), [3](#), [7](#), [8](#)
- [10] Runyu Ding, Jihan Yang, Chuhui Xue, Wenqing Zhang, Song Bai, and Xiaojuan Qi. Pla: Language-driven open-vocabulary 3d scene understanding. In *International Conference on Computer Vision and Pattern Recognition (CVPR)*, 2023. [2](#)
- [11] Pedro Felzenszwalb and Daniel Huttenlocher. Efficient graph-based image segmentation. *International Journal of Computer Vision*, 59:167–181, 2004. [5](#)
- [12] Benjamin Graham, Martin Engelcke, and Laurens van der Maaten. 3d semantic segmentation with submanifold sparse convolutional networks. In *International Conference on Computer Vision and Pattern Recognition (CVPR)*, 2018. [3](#)
- [13] Yining Hong, Zishuo Zheng, Peihao Chen, Yian Wang, Junyan Li, Zhenfang Chen, and Chuang Gan. Multiply: A multisensory object-centric embodied large language model in 3d world. In *International Conference on Computer Vision and Pattern Recognition (CVPR)*, 2024. [2](#)
- [14] Binh-Son Hua, Quang-Hieu Pham, Duc Thanh Nguyen, Minh-Khoi Tran, Lap-Fai Yu, and Sai-Kit Yeung. Scenenn: A scene meshes dataset with annotations. In *2016 Fourth International Conference on 3D Vision (3DV)*, pages 92–101, 2016. [2](#), [3](#)
- [15] Haifeng Huang, Yilun Chen, Zehan Wang, Rongjie Huang, Runsen Xu, Tai Wang, Luping Liu, Xize Cheng, Yang Zhao, Jiangmiao Pang, and Zhou Zhao. Chat-scene: Bridging 3d scene and large language models with object identifiers. In *International Conference on Neural Information Processing Systems (NeurIPS)*, 2024. [2](#)
- [16] Rui Huang, Songyou Peng, Ayca Takmaz, Federico Tombari, Marc Pollefeys, Shiji Song, Gao Huang, and Francis Engelmann. Segment3d: Learning fine-grained class-agnostic 3d segmentation without manual labels. *European Conference on Computer Vision (ECCV)*, 2024. [5](#)
- [17] Marcelo Jacinto, João Pinto, Jay Patrikar, John Keller, Rita Cunha, Sebastian Scherer, and António Pascoal. Pegasus simulator: An isaac sim framework for multiple aerial vehicles simulation. In *2024 International Conference on Unmanned Aircraft Systems (ICUAS)*, 2024. [4](#)
- [18] Baoxiong Jia, Yixin Chen, Huangyue Yu, Yan Wang, Xuesong Niu, Tengyu Liu, Qing Li, and Siyuan Huang. Sceneverse: Scaling 3d vision-language learning for grounded scene understanding. *European Conference on Computer Vision (ECCV)*, 2024. [2](#)
- [19] Hanxiao Jiang, Yongsan Mao, Manolis Savva, and Angel X Chang. Opd: Single-view 3d openable part detection. In *European Conference on Computer Vision (ECCV)*, 2022. [3](#)
- [20] Zhenyu Jiang, Cheng-Chun Hsu, and Yuke Zhu. Ditto: Building digital twins of articulated objects from interaction. In *International Conference on Computer Vision and Pattern Recognition (CVPR)*, 2022. [3](#)
- [21] Mahfud Jiono and Hsien-I Lin. Software framework of autonomous mobile robots on isaac sim and ros. In *2023 11th International Conference on Control, Mechatronics and Automation (ICCMA)*, 2023. [4](#)
- [22] Arno Knapitsch, Jaesik Park, Qian-Yi Zhou, and Vladlen Koltun. Tanks and temples: benchmarking large-scale scene reconstruction. *ACM Trans. Graph.*, 2017. [5](#)
- [23] Haoran Li, Haolin Shi, Wenli Zhang, Wenjun Wu, Yong Liao, Lin Wang, Lik-hang Lee, and Pengyuan Zhou. Dreamscene: 3d gaussian-based text-to-3d scene generation via formation pattern sampling. In *European Conference on Computer Vision (ECCV)*, 2024. [2](#)

- [24] Jiayi Liu, Ali Mahdavi-Amiri, and Manolis Savva. Paris: Part-level reconstruction and motion analysis for articulated objects. In *International Conference on Computer Vision (ICCV)*, 2023. 3
- [25] Jiayi Liu, Hou In Ivan Tam, Ali Mahdavi-Amiri, and Manolis Savva. Cage: Controllable articulation generation. In *International Conference on Computer Vision and Pattern Recognition (CVPR)*, 2024. 3
- [26] L. Liu, Wenqiang Xu, Haoyuan Fu, Sucheng Qian, Yong-Jin Han, and Cewu Lu. Akb-48: A real-world articulated object knowledge base. In *International Conference on Computer Vision and Pattern Recognition (CVPR)*, 2022. 3
- [27] Cewu Lu, Hao Su, Yonglu Li, Yongyi Lu, Li Yi, Chi-Keung Tang, and Leonidas J. Guibas. Beyond holistic object recognition: Enriching image understanding with part states. In *International Conference on Computer Vision and Pattern Recognition (CVPR)*, 2018. 3
- [28] Arjun Majumdar, Anurag Ajay, Xiaohan Zhang, Pranav Putta, Sriram Yenamandra, Mikael Henaff, Sneha Silwal, Paul Mcvay, Oleksandr Maksymets, Sergio Arnaud, Karmesh Yadav, Qiyang Li, Ben Newman, Mohit Sharma, Vincent Berges, Shiqi Zhang, Pulkit Agrawal, Yonatan Bisk, Dhruv Batra, Mrinal Kalakrishnan, Franziska Meier, Chris Paxton, Sasha Sax, and Aravind Rajeswaran. Openeqa: Embodied question answering in the era of foundation models. In *International Conference on Computer Vision and Pattern Recognition (CVPR)*, 2024. 2
- [29] Yongsan Mao, Yiming Zhang, Hanxiao Jiang, Angel X Chang, and Manolis Savva. Multiscan: Scalable rgb-d scanning for 3d environments with articulated objects. 2022. 2, 3, 4, 5, 7, 8
- [30] Kaichun Mo, Shilin Zhu, Angel X. Chang, Li Yi, Subarna Tripathi, Leonidas J. Guibas, and Hao Su. PartNet: A large-scale benchmark for fine-grained and hierarchical part-level 3D object understanding. In *International Conference on Computer Vision and Pattern Recognition (CVPR)*, 2019. 2
- [31] Soroush Nasiriany, Abhiram Maddukuri, Lance Zhang, Adeet Parikh, Aaron Lo, Abhishek Joshi, Ajay Mandlekar, and Yuke Zhu. Robocasa: Large-scale simulation of everyday tasks for generalist robots. In *Robotics: Science and Systems (RSS)*, 2024. 3
- [32] Giang Hoang Nguyen, Daniel Beßler, Simon Stelter, Mihai Pomarlan, and Michael Beetz. Translating universal scene descriptions into knowledge graphs for robotic environment. In *International Conference on Robotics and Automation (ICRA)*, 2024. 3, 4
- [33] Phuc D. A. Nguyen, Tuan Duc Ngo, Evangelos Kalogerakis, Chuang Gan, Anh Tran, Cuong Pham, and Khoi Nguyen. Open3dis: Open-vocabulary 3d instance segmentation with 2d mask guidance. In *International Conference on Computer Vision and Pattern Recognition (CVPR)*, 2024. 5
- [34] NVIDIA. NVIDIA Isaac Sim. <https://developer.nvidia.com/isaac-sim>, . Accessed: 2024-14-11. 4
- [35] NVIDIA. NVIDIA USD Code. <https://docs.api.nvidia.com/nim/reference/nvidia-usdcode-llama3-70b-instruct>, . Accessed: 2024-14-11. 4
- [36] NVIDIA. NVIDIA USD Search. [api.nvidia.com/nim/reference/nvidia-usdsearch](https://docs.api.nvidia.com/nim/reference/nvidia-usdsearch), . Accessed: 2024-14-11. 4
- [37] Başak Melis Öcal, Maxim Tatarchenko, Sezer Karaoglu, and Theo Gevers. Sceneteller: Language-to-3d scene generation. 2024. 2
- [38] OpenAI. GPT-4o mini: advancing cost-efficient intelligence. <https://openai.com/index/gpt-4o-mini-advancing-cost-efficient-intelligence/>, 2024. Accessed: 2024-14-11. 14
- [39] OpenAI. Hello GPT-4o. <https://openai.com/index/hello-gpt-4o/>, 2024. Accessed: 2024-14-11. 14
- [40] Songyou Peng, Kyle Genova, Chiyu "Max" Jiang, Andrea Tagliasacchi, Marc Pollefeys, and Thomas Funkhouser. Openscene: 3d scene understanding with open vocabularies. In *International Conference on Computer Vision and Pattern Recognition (CVPR)*, 2023. 5
- [41] Mihir Prabhudesai, Hsiao-Yu Fish Tung, Syed Ashar Javed, Maximilian Sieb, Adam W. Harley, and Katerina Fragkiadaki. Embodied Language Grounding With 3D Visual Feature Representations . In *International Conference on Computer Vision and Pattern Recognition (CVPR)*, 2020. 2
- [42] Shengyi Qian, Linyi Jin, Chris Rockwell, Siyi Chen, and David F. Fouhey. Understanding 3d object articulation in internet videos. In *International Conference on Computer Vision and Pattern Recognition (CVPR)*, 2022. 3
- [43] Alexander Raistrick, Lingjie Mei, Karhan Kayan, David Yan, Yiming Zuo, Beining Han, Hongyu Wen, Meenal Parakh, Stamatis Alexandropoulos, Lahav Lipson, Zeyu Ma, and Jia Deng. Infinigen indoors: Photorealistic indoor scenes using procedural generation. In *International Conference on Computer Vision and Pattern Recognition (CVPR)*, 2024. 4
- [44] Santhosh Kumar Ramakrishnan, Aaron Gokaslan, Erik Wijmans, Oleksandr Maksymets, Alexander Clegg, John M Turner, Eric Undersander, Wojciech Galuba, Andrew Westbury, Angel X Chang, Manolis Savva, Yili Zhao, and Dhruv Batra. Habitat-matterport 3d dataset (HM3d): 1000 large-scale 3d environments for embodied AI. In *International Conference on Neural Information Processing Systems (NeurIPS)*, 2021. 2
- [45] Maximiliano Rojas, Gabriel Hermosilla, Daniel Yunge, and Gonzalo Farias. An easy to use deep reinforcement learning library for ai mobile robots in isaac sim. *Applied Sciences*, 2022. 4
- [46] David Rozenberszki, Or Litany, and Angela Dai. Unscene3d: Unsupervised 3d instance segmentation for indoor scenes. In *International Conference on Computer Vision and Pattern Recognition (CVPR)*, 2024. 3
- [47] Sayan Deb Sarkar, Ondrej Miksik, Marc Pollefeys, Daniel Barath, and Iro Armeni. Sgaligner : 3d scene alignment with scene graphs, 2023. 15
- [48] Gianluca Scarpellini, Stefano Rosa, Pietro Morerio, Lorenzo Natale, and Alessio Del Bue. Look around and learn: Self-training object detection by exploration. In *European Conference on Computer Vision (ECCV)*, 2024. 2
- [49] Jonas Schult, Francis Engelmann, Alexander Hermans, Or Litany, Siyu Tang, and Bastian Leibe. Mask3d: Mask trans-

- former for 3d semantic instance segmentation. In *International Conference on Robotics and Automation (ICRA)*, 2023. 2, 3, 6
- [50] Thomas Schöps, Johannes L. Schönberger, Silvano Galliani, Torsten Sattler, Konrad Schindler, Marc Pollefeys, and Andreas Geiger. A multi-view stereo benchmark with high-resolution images and multi-camera videos. In *International Conference on Computer Vision and Pattern Recognition (CVPR)*, 2017. 5
- [51] Yahao Shi, Xinyu Cao, and Bin Zhou. Self-supervised learning of part mobility from point cloud sequence. *Computer Graphics Forum*, 2020. 3
- [52] Yahao Shi, Xinyu Cao, Feixiang Lu, and Bin Zhou. P3-net: Part mobility parsing from point cloud sequences via learning explicit point correspondence. In *AAAI Conference on Artificial Intelligence*, 2022. 3
- [53] Chaoyue Song, Jiacheng Wei, Chuan Sheng Foo, Guosheng Lin, and Fayao Liu. Reacto: Reconstructing articulated objects from a single video. In *International Conference on Computer Vision and Pattern Recognition (CVPR)*, 2024. 3
- [54] Julian Straub, Thomas Whelan, Lingni Ma, Yufan Chen, Erik Wijmans, Simon Green, Jakob J. Engel, Raul Mur-Artal, Carl Ren, Shobhit Verma, Anton Clarkson, Mingfei Yan, Brian Budge, Yajie Yan, Xiaqing Pan, June Yon, Yuyang Zou, Kimberly Leon, Nigel Carter, Jesus Briales, Tyler Gillingham, Elias Mueggler, Luis Pesqueira, Manolis Savva, Dhruv Batra, Hauke M. Strasdat, Renzo De Nardi, Michael Goesele, Steven Lovegrove, and Richard Newcombe. The Replica dataset: A digital replica of indoor spaces. *arXiv preprint arXiv:1906.05797*, 2019. 3
- [55] Xiaohao Sun, Hanxiao Jiang, Manolis Savva, and Angel Chang. Opdmulti: Openable part detection for multiple objects. In *International Conference on 3D Vision (3DV)*, 2024. 3, 7
- [56] Archana Swaminathan, Anubhav Gupta, Kamal Gupta, Shishira R. Maiya, Vatsal Agarwal, and Abhinav Shrivastava. Leia: Latent view-invariant embeddings for implicit 3d articulation. In *European Conference on Computer Vision (ECCV)*, 2024. 3
- [57] Ayça Takmaz, Elisabetta Fedele, Robert W. Sumner, Marc Pollefeys, Federico Tombari, and Francis Engelmann. OpenMask3D: Open-Vocabulary 3D Instance Segmentation. In *International Conference on Neural Information Processing Systems (NeurIPS)*, 2023. 3, 5
- [58] Gül Varol, Javier Romero, Xavier Martin, Naureen Mahmood, Michael J. Black, Ivan Laptev, and Cordelia Schmid. Learning from synthetic humans. In *International Conference on Computer Vision and Pattern Recognition (CVPR)*, 2017. 3
- [59] Petar Veličković, Guillem Cucurull, Arantxa Casanova, Adriana Romero, Pietro Liò, and Yoshua Bengio. Graph attention networks, 2018. 15
- [60] Marcel Torne Villasevil, Anthony Simeonov, Zechu Li, April Chan, Tao Chen, Abhishek Gupta, and Pulkit Agrawal. Reconciling Reality through Simulation: A Real-To-Sim-to-Real Approach for Robust Manipulation. In *Proceedings of Robotics: Science and Systems*, 2024. 2, 3, 4
- [61] Thang Vu, Kookhoi Kim, Tung M. Luu, Xuan Thanh Nguyen, and Chang D. Yoo. Softgroup for 3d instance segmentation on 3d point clouds. In *International Conference on Computer Vision and Pattern Recognition (CVPR)*, 2022. 3, 6, 7, 16
- [62] Johanna Wald, Armen Avetisyan, Nassir Navab, Federico Tombari, and Matthias Niessner. Rio: 3d object instance re-localization in changing indoor environments. In *International Conference on Computer Vision (ICCV)*, 2019. 2, 3
- [63] Qi Wang, Ruijie Lu, Xudong Xu, Jingbo Wang, Michael Yu Wang, Bo Dai, Gang Zeng, and Dan Xu. Roomtex: Texturing compositional indoor scenes via iterative inpainting. In *European Conference on Computer Vision (ECCV)*, 2024. 2
- [64] Tai Wang, Xiaohan Mao, Chenming Zhu, Runsen Xu, Ruiyuan Lyu, Peisen Li, Xiao Chen, Wenwei Zhang, Kai Chen, Tianfan Xue, Xihui Liu, Cewu Lu, Dahua Lin, and Jiangmiao Pang. Embodiedscan: A holistic multi-modal 3d perception suite towards embodied ai. In *International Conference on Computer Vision and Pattern Recognition (CVPR)*, 2024. 2
- [65] Xiaogang Wang, Bin Zhou, Yahao Shi, Xiaowu Chen, Qingping Zhao, and Kai Xu. Shape2motion: Joint analysis of motion parts and attributes from 3d shapes. *International Conference on Computer Vision and Pattern Recognition (CVPR)*, 2019. 3
- [66] Zijie Wu, Mingtao Feng, Yaonan Wang, He Xie, Weisheng Dong, Bo Miao, and Ajmal Mian. External knowledge enhanced 3d scene generation from sketch. In *European Conference on Computer Vision (ECCV)*, 2024. 2
- [67] Fanbo Xiang, Yuzhe Qin, Kaichun Mo, Yikuan Xia, Hao Zhu, Fangchen Liu, Minghua Liu, Hanxiao Jiang, Yifu Yuan, He Wang, Li Yi, Angel X. Chang, Leonidas J. Guibas, and Hao Su. SAPIEN: A simulated part-based interactive environment. In *International Conference on Computer Vision and Pattern Recognition (CVPR)*, 2020. 3
- [68] Karmesh Yadav, Ram Ramrakhya, Santhosh Kumar Ramakrishnan, Theo Gervet, John Turner, Aaron Gokaslan, Noah Maestre, Angel Xuan Chang, Dhruv Batra, Manolis Savva, et al. Habitat-matterport 3d semantics dataset. In *International Conference on Computer Vision and Pattern Recognition (CVPR)*, 2023. 2
- [69] Zihao Yan, Ruizhen Hu, Xingguang Yan, Luanmin Chen, Oliver van Kaick, Hao Zhang, and Hui Huang. Rpm-net: Recurrent prediction of motion and parts from point cloud. *ACM Transactions on Graphics*, 2019. 3
- [70] Yunseo Yang, Jihun Kim, and Kuk-Jin Yoon. Syn-to-real domain adaptation for point cloud completion via part-based approach. In *European Conference on Computer Vision (ECCV)*, 2024. 2
- [71] Yue Yang, Fan-Yun Sun, Luca Weihs, Eli VanderBilt, Alvaro Herrasti, Winson Han, Jiajun Wu, Nick Haber, Ranjay Krishna, Lingjie Liu, Chris Callison-Burch, Mark Yatskar, Aniruddha Kembhavi, and Christopher Clark. Holodeck: Language guided generation of 3d embodied ai environments. *International Conference on Computer Vision and Pattern Recognition (CVPR)*, 2024. 2

- [72] Lei Yao, Yi Wang, Moyun Liu, and Lap-Pui Chau. Sgi-former: Semantic-guided and geometric-enhanced interleaving transformer for 3d instance segmentation, 2024. [3](#)
- [73] Chandan Yeshwanth, Yueh-Cheng Liu, Matthias Nießner, and Angela Dai. Scannet++: A high-fidelity dataset of 3d indoor scenes. In *International Conference on Computer Vision (ICCV)*, 2023. [2](#), [3](#), [4](#), [5](#), [6](#), [8](#), [13](#), [14](#), [16](#)
- [74] Vicky Zeng, Tabitha Edith Lee, Jacky Liang, and Oliver Kroemer. Visual identification of articulated object parts. In *IEEE/RSJ International Conference on Intelligent Robots and Systems (IROS)*, 2021. [3](#)
- [75] Guanyao Zhai, Evin Pinar Örnek, Shun-Cheng Wu, Yan Di, Federico Tombari, Nassir Navab, and Benjamin Busam. Commonsences: Generating commonsense 3d indoor scenes with scene graphs. In *International Conference on Neural Information Processing Systems (NeurIPS)*, 2023. [2](#)
- [76] Zhehua Zhou, Jiayang Song, Xuan Xie, Zhan Shu, Lei Ma, Dikai Liu, Jianxiong Yin, and Simon See. Towards building ai-cps with nvidia isaac sim: An industrial benchmark and case study for robotics manipulation. In *Proceedings of the 46th International Conference on Software Engineering: Software Engineering in Practice*, 2024. [4](#)

Holistic Understanding of 3D Scenes as Universal Scene Description

Supplementary Material

We provide additional details on:

- the training process of annotators (Sec. 7),
- the statistics of Articulate3D (Sec. 8),
- example use case with Articulate3D (Sec. 9),
- connectivity graph prediction (Sec. 10),
- experiment details and additional results (Sec. 11).

7. Annotators Training

To ensure the quality and consistency of annotations, annotators underwent comprehensive training supported by detailed documentation and tutorials. The preparation materials included:

Segmentation Training:

- Two training videos, totaling 40 minutes, covering the segmentation tool, illustrative examples of typical cases and exceptions.
- Documentation with examples for all object classes in the fixed object label list, including: (1) images of segmented parts, (2) their corresponding connectivity graphs, and (3) the step-by-step sequence of commands used to achieve precise segmentation.
- A complete guide to the application’s controls and shortcuts.

Articulation Training:

- A 15-minute training video demonstrating the articulation annotation tool and process, with examples of rotation and translation articulations.
- Documentation with examples of the different articulated parts classes.

Additionally, annotators were provided with chat support throughout the annotation process. The chat support was especially valuable during the initial review phase, allowing annotators to resolve questions, particularly around complex connectivity graphs, e.g., oven models, where controls are physically attached to the oven door but semantically part of the oven body.

8. Dataset Statistics

For a comprehensive overview of the annotated object and part labels, we refer to Fig. 6 and Fig. 7, which provide information both on the labels and on their distributions.

We note that the dataset also includes additional labels to address variations based on location (e.g., "cabinet" versus "wardrobe"), functional mechanisms (e.g., "faucet handle" versus "faucet ventill"), and other contextual distinctions which are not captured in the provided figures. We will include resources for mapping these additional labels and their parent categories with the dataset release.

We also provide size information for the annotated items (both objects and parts) in Fig. 8, where size is measured by the faces (triangles) count of each item. Our analysis reveals that Articulate3D includes a mix of large objects and many smaller ones with only a few faces. This highlights both the high quality of the annotations in capturing intricate details, as well as the variability within the dataset.

Our statistical analysis focuses solely on annotations added by our annotators. Since our work builds upon the ScanNet++ dataset [73], we ensure full compatibility between our annotations and those from ScanNet++. Unaltered ScanNet++ annotations (e.g., walls, floors, and sofas) are directly integrated into the final USD, while certain labels, such as "cabinet," are entirely replaced by our own annotations, as illustrated in Fig. 5. We will provide a script merging the annotations from Articulate3D and ScanNet++.

8.1. Segmentations Quality Evaluation

To assess the quality of our segmentation annotations, we conducted a control experiment involving two annotators. They were each tasked with re-annotating a "control scene"—a scene that had been previously annotated, then reviewed, and approved by the sixth annotator. The annotations were manually matched item-by-item between the two annotators, and IoU was calculated for each matched pair. The average IoU across all items was used to evaluate the scene. Importantly, we ensured that the annotators performing the re-annotations were not the original annotators for these scenes. We achieved an IoU of 0.93 for the control scene.

9. Use Case: USD Scene Insertion

We present a pipeline for automated, semantically-aware object insertion into USD scenes. Given a USD scene from Articulate3D, a 3D object file, and the object’s label, our solution produces a new USD scene with the object placed in a semantically-appropriate location. For example, in a bedroom scene, a pillow object would be placed on a bed, while in an office scene, a bottle would be placed on a desk. The pipeline uses a LLM to show the USD-understanding capabilities of LLMs, as well as to minimize user involvement. Implementation details are outlined below.

The method requires three inputs: (1) a USD Articulate3D scene, (2) a 3D object file, and (3) the object’s label. We support various 3D file formats (e.g., OBJ, USD, GLB). Given the inputs, the pipeline extracts item labels and connectivity data from the USD scene and prompts the LLM to



Figure 5. Overview of the annotations provided by Articulate3D, ScanNet++ [73], and their combination. Articulate3D offers (a) detailed annotations at both the object and part levels, including connectivity information, and (b) full articulation annotations. By combining ScanNet++ with Articulate3D, users gain a comprehensive scene segmentation with nearly 100% coverage, alongside detailed annotations for interactable objects and their motion specifications.

determine the appropriate placement target (e.g., a bed for the pillow) and the type of surface required (e.g., horizontal for a pillow, vertical for a poster). With this information, the pipeline employs RANSAC to identify a suitable placement plane on the target object. Using the plane, the input object, and an example USD insertion script defined by us, the LLM generates a script customized for the specific insertion case. The generated script is then executed to produce the updated Articulate3D USD scene.

For our pipeline, we have tested two LLMs - GPT-4o

mini [38] and GPT-4o [39], both producing the desired results. We will release the pipeline as a Python CLI library.

10. Connectivity Prediction

To show the value of Articulate3D in 3D holistic scene understanding, particularly in the context of connectivity graphs within articulated objects, we conduct experiments on the task of connectivity graph prediction. As introduced in Sec. 4.2, a connectivity graph refers to the hierarchies between different partegments. In the graph, the "root" part is

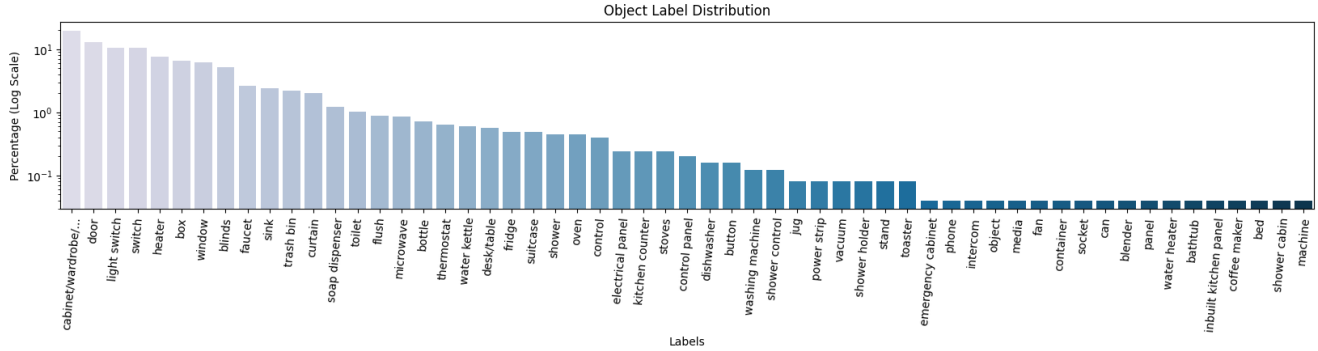


Figure 6. Distribution of the object-level labels.

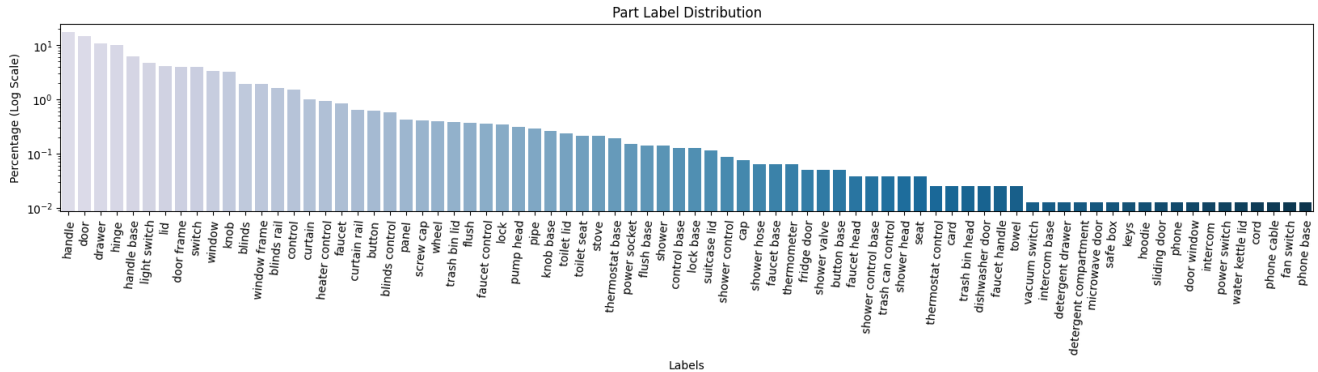


Figure 7. Distribution of the part-level labels.

the base to which other parts are attached. A "child" refers to a part that belongs to the parent part. We train a network on Articulate3D that takes the 3D point cloud of objects' parts as input and predicts the connectivity graph of the parts by inferring relationship between each part pair.

10.1. Method

We draw inspiration from the existing scene-graph-based framework [47] and apply a similar network for the task. As shown in Fig. 10, PointNet [3] is applied to extract the information of geometry and appearance of part segments, outputting per-part feature vectors. Then we treat each part segment as a node and feed the feature vectors into a graph attention network [59] to extract the relationship between the nodes. The features of the two node are concatenated and fed into a MLP to infer the pairwise relationship between them ($\{no\ relationship, parent\ of, child\ of\}$).

10.2. Result

In Table. 7, we show the accuracy of the connectivity graph prediction. From the table we can see that (1) the random guess could achieve 36% accuracy of edge prediction by randomly picking one relationship from $\{no\ relationship, parent\ of, child\ of\}$ for each pair of part segments, and (2) it has poor performance in the connectivity graph prediction for objects as only 6.1% of

objects' connectivity graph are correctly predicted. Compared to the random guess, by training on Articulate3D, our network can achieve much better performance in both edge prediction (72.7%) and connectivity graph prediction (31.1%).

In order to further understand the performance of our model in connectivity or edge prediction, we plot the ROC curves as shown in Fig. 9. As the edge prediction is a 3-category classification problem, we transform the results into two binary classification problems for straightforward ROC plot: connectivity classification ($\{no\ relationship, \{parent\ of, child\ of\}\}$) and hierarchical classification ($\{parent\ of, child\ of\}$). From Fig. 9 we can see that our model has good performance (with 0.88) in predicting the hierarchical relationship between part segments (whether a is the parent of b or the opposite), while it is more challenging to tell whether two parts have hierarchies within the connectivity graph (AUC 0.74).

10.3. Future Application

This section shows that apart from articulation prediction as introduced in Sec. 5, Articulate3D also enables connectivity graph prediction, which is the core component of USD format for scene representations. Together with our benchmarks of articulation predictions, Articulate3D lays

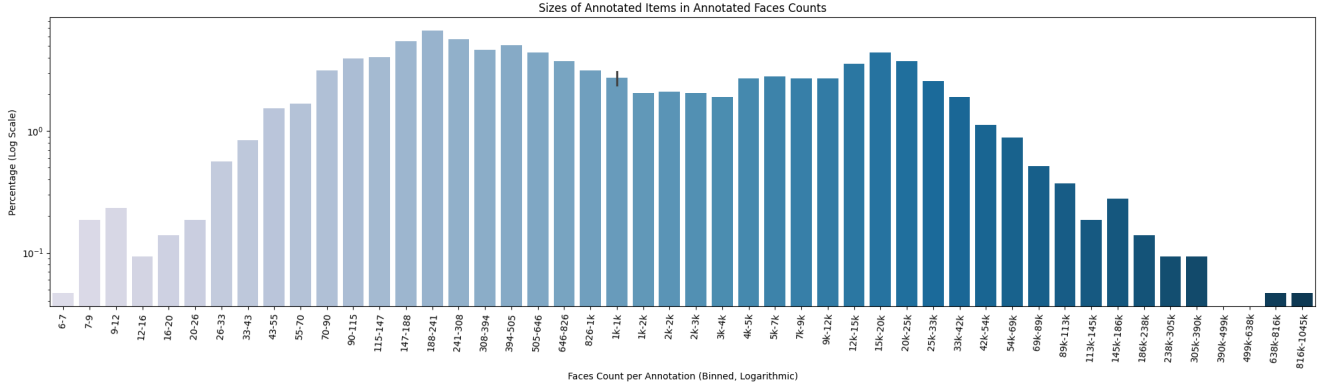


Figure 8. Distribution of face counts per annotated item using logarithmic binning. Articulate3D features numerous high-detail small annotations alongside larger objects

Method	Acc_{edge} (%)	Acc_{obj} (%)
Random	36.0	6.1
Ours	72.7	31.1

Table 7. Accuracy of connectivity graph prediction. Acc_{edge} represents the percentage of edges that are correctly recognized in $\{no\ relationship, parent\ of, child\ of\}$; Acc_{obj} represents the percentage of objects that has correct connectivity graph with all the edges within it correctly recognized.

the foundation for 3D holistic scene understanding in the USD format by allowing training of the models that can predict both articulations and connectivity graphs, bearing great potentials in downstream applications.

11. Experiment Details and Additional Results

This section introduces the implementation details of the experiments in Sec. 5 and additional results.

11.1. Implementation Details

We take 15% of the scenes (42 scenes) in Articulate3D as the test set for evaluations. For the training and evaluation of all the methods, we downsample the point cloud with a voxel size of 2cm from the original laser scans in [73], in order to achieve balance between preserving geometric details and computation resources. For the task of movable part segmentation, all points in the scene will be semantically segmented into one of the classes $\{background, rotation, translation\}$. For points of $\{rotation, translation\}$, instance labels are furthered assigned for instance segmentation of movable part.

Softgroup[†]. As described in the main paper, we adopt the framework of Softgroup[61] for this task. We firstly pre-train Softgroup[61] for 2000 epochs in the task of semantic segmentation, and then further train the semantic segmentation network together with instance grouping branch for

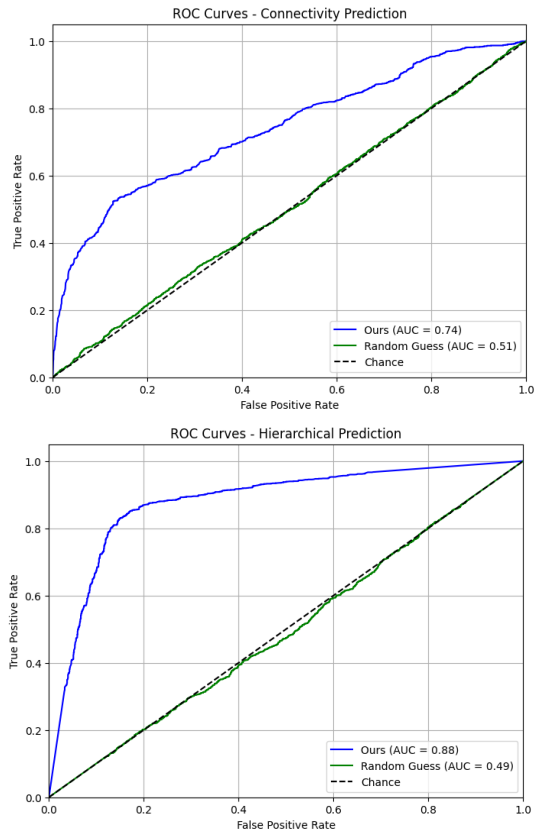


Figure 9. ROC curve of connectivity and hierarchical relationship of part segments prediction of our method.

movable part segmentation and the articulation branch for articulation parameters prediction for 220 epochs. For interactive part segmentation, we also pretrain the network with semantic segmentation for 2000 epochs and then another 360 epochs for instance segmentation of interactive parts. The training batch size is 6, on 2 NVIDIA A100-40g GPUs. Learning rate is 0.002.

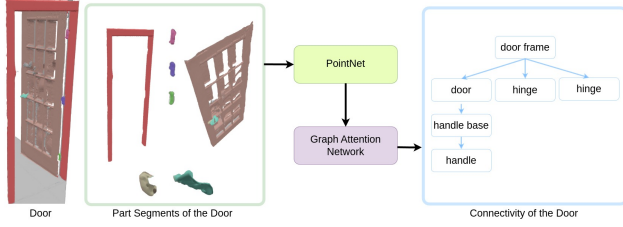


Figure 10. Connectivity Graph Prediction of Parts of Articulated Objects.

Mask3D[†]. For Mask3D[†], we firstly pretrain it for semantic-instance segmentation of movable part for 1000 epochs and then further train it for joint tasks of movable part segmentation and articulation prediction for 920 epochs. For interactable part segmentation, we train the network for 1400 epochs. The training batch size is 1, on 1 NVIDIA A100-40g Gpu and the learning rate is 0.0001. In order that the input of large scenes in Articulate3D fits in the memory of the training GPU, we randomly crop the input scenes into a $6 \times 6 m^2$ cuboid during training.

ArtMask3D. Similar to Mask3D[†], we also train ArtMask3D with the semantic-instance segmentation of movable part for 1160 epochs and then further train it for joint prediction of movable parts and articulation parameters for 680 epochs. For interactable part segmentation, we train ArtMask3D for 640 epochs. The training batch size is 1, on 1 NVIDIA A100-40g GPU and the learning rate is 0.0001. The crop size is $6 \times 6 m^2$ in cuboid during training.

11.2. Additional Results

In order to further understand the performance of the proposed ArtMask3D, we analyze its performance across objects of various sizes and categories. In Fig. 11, we show the performance of ArtMask3D in the task of movable part segmentation and articulation parameter prediction over the movable parts with different number of points. From the figure we can see that for the task of movable part segmentation and articulation origin prediction, ArtMask3D performs better with middle-sized parts (with 1739 ~ 5207 points) than with the small or large parts (less than 1739 or more than 5207 points). On the other hand, articulation axis prediction is more challenging than origin prediction for the small- and middle-sized objects.

We also show the performance of ArtMask3D across the movable parts of different semantic categories. We select 6 dominant categories with significant numbers in both training and test set. In Fig. 12, we can see that ArtMask3D performs better in the category of drawer (middle sized objects) than the other categories (small and large objects), which is in accordance with the results shown in Fig. 11. It is noticeable that ArtMask3D fails in the prediction of all the faucets, which is mainly because the 3D meshes of faucets are not well reconstructed and incomplete due to the com-

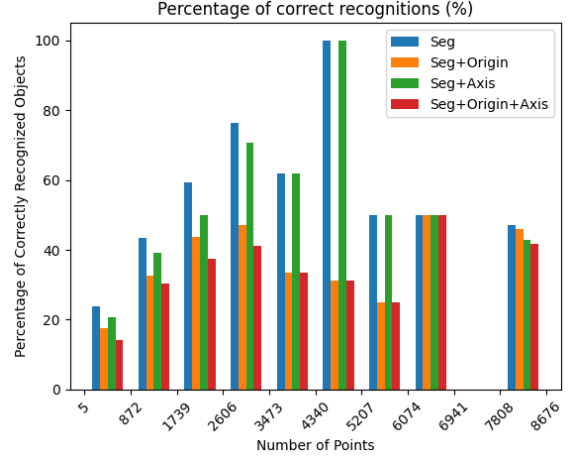


Figure 11. Percentage of correct recognitions v.s. size of movable parts

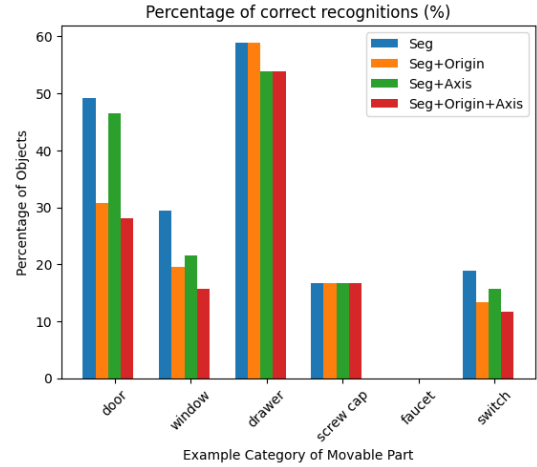


Figure 12. Percentage of correct recognitions v.s. categories of movable parts

plicated geometry and reflective surfaces of them.